Medium effect on photon production in ultrarelativistic nuclear collisions

Chung-sik Song* and George Fai†
Center for Nuclear Research, Department of Physics, Kent State University, Kent, Ohio 44242
(Received 23 February 1998)

The effect of in-medium vector and axial-vector meson masses on photon production is studied. We assume that the effective mass of a vector meson in hot nuclear matter decreases according to a universal scaling law, while that of an axial-vector meson is given by Weinberg's mass formula. We find that the thermal production rate of photons increases with reduced masses, and is enhanced by an order of magnitude at $T=160$ MeV with $m_\rho=300$ MeV. Assuming a hydrodynamic evolution, we estimate the effect of the reduced masses on photon production in nucleus-nucleus collisions. The result is compared to experimental data from the WA80/WA98 Collaboration. [S0556-2813(98)03109-4]

PACS number(s): 25.75.−q, 24.85.+p, 12.38.Mh

I. INTRODUCTION

For hadronic matter at sufficiently high temperature and/or density, we expect a phase transition into a locally thermalized, deconfined plasma of quarks and gluons, the so-called quark-gluon plasma (QGP) [1]. Chiral symmetry, spontaneously broken in the ground state of quantum chromodynamics (QCD), is expected to be restored under such extreme conditions as shown by numerical simulations on the lattice [2]. These properties of QCD are of great interest in order to understand the behavior of strongly interacting particles. High energy nucleus-nucleus collisions offer a unique opportunity to explore the properties of QCD, in particular its phase structure, at high temperatures and densities [3].

Photon and lepton pair production have been suggested more than 20 years ago as promising probes to study the properties of hot dense matter in high energy nucleus-nucleus collisions [4]. The strong temperature dependence of the production rate of these signals makes them potential tools that can hopefully discriminate the various states of hadronic matter with different temperatures. In addition, these signals carry information on the hot dense matter without further distortion, since these electromagnetic probes interact very weakly with surrounding particles. However, most model calculations show that the hadronic contributions dominate the signals from quark-gluon plasma [5,6]. This implies that the bulk of the photon or dilepton spectra observed in experiments will provide information on the properties of the hadronic phase under extreme conditions but below (or at most at) the phase transition temperature and/or density.

Recent interest in dileptons with a low invariant mass has been sparked by the experimental data from the CERES Collaboration [7], which show a considerable enhancement at invariant masses of about 500 MeV for super proton synchrotron (SPS)-energy S+Au collisions as compared to proton-proton and proton-nucleus collisions. A similar enhancement has also been seen by the HELIOS Collaboration at a more forward rapidity [8]. It is noteworthy that there is also an enhancement at energies above the ρ peak in these data [3]. Suggestions have been made that the excess dileptons seen in these experiments are from pion-pion annihilation, $\pi^+\pi^-\to e^+e^-$. However, model calculations that have taken this channel into account can at best reach the lower end of the sum of statistical and systematic errors of the CERES data in the low invariant mass region [9]. For the HELIOS results, which are unfortunately given without a systematic error, there is still a disagreement by up to 50% between the data and the calculations around an invariant mass of 500 MeV [9]. It is, therefore, interesting to see to what extent medium corrections modify dilepton production. It has been suggested that the enhancement may be because of the dropping of the vector meson masses at finite temperature and density [10], as proposed in Ref. [11], and/or to the broadening of vector meson resonances by the many-body effects in dense matter [12]. However, more conservative effects, such as a modified in-medium pion dispersion relation [13] or secondary mesonic scattering [14], may also give dilepton enhancement.

In this paper we consider the medium effects on photon production at SPS heavy-ion collisions. In particular, we concentrate on the effects of dropping vector and axial-vector meson masses on photon production. The result is compared to recent measurements of the WA80 Collaboration that provide an upper limit for photon production in hot and dense matter [15], and to the preliminary results of the WA98 Collaboration [3]. It has been shown that these experimental data can be well described by the hadronic contributions without any medium effect [16]. Thus, it is very interesting and valuable to see whether the medium effects, which play an important role in dilepton production are also consistent with the photon spectra. Steele *et al.* have calculated dilepton and photon emission rates from a hadron gas from this perspective, using chiral reduction formulas [17]. Sarkar *et al.* have recently discussed photon production rates in the framework of an effective Lagrangian description along the lines of quantum hadrodynamics [18]. Halász *et al.* study photon production from the perspective of the hidden local symmetry approach and use several parametrized scenarios inspired by this approach in a relativistic transport model [19]. A calculation that incorporates the change of hadron masses in dense matter self-consistently has been carried out with the help of the same transport model [20]. Nonthermal direct photon production has also been discussed

*Electronic address: csong@cnrred.kent.edu
†Electronic address: fai@cnrred.kent.edu

recently in the ultrarelativistic quantum molecular dynamics (UrQMD) framework [21]. In contrast, the present paper uses thermal equilibrium and a simple fluid-dynamical picture. We do not attempt to calculate the effective mass of the vector meson from first principles, but apply two physically motivated parametrizations and use the standard Weinberg formula [22] for the effective mass of the axial-vector meson.

With respect to comparing to SPS data, the most important omission of this paper is probably that the central rapidity region is considered approximately baryon free. The baryonic contribution to photon production is usually neglected in fluid-dynamical calculations, and the magnitude of the effect was assessed in Refs. [17] and [20]. Note that the photon yield from baryons is very sensitive to the initial nucleon density and that the largest baryonic contributions come at low transverse momenta. The present approximation is sufficient to study the effect of dropping vector and axial-vector masses, which is the main focus of this investigation.

In the following section, we study the effect of the in-medium vector and axial-vector meson masses on the thermal production rates of photons. We assume that the vector meson mass is reduced according to a universal scaling law and the axial-vector meson masses are given by Weinberg's mass formula [22]. We include these medium effects in a dynamical model calculation which simulates the evolution of hot dense matter produced in nucleus-nucleus collisions in Sec. III. We consider a one-dimensional hydrodynamic expansion for the hot dense matter with Bjorken's initial conditions [23]. We study cases with and without a first-order phase transition. The medium effect gives different initial temperatures, phase-transition temperatures, and mixed-phase lifetimes for the two different scenarios. In the Appendix, we summarize thermal production rates for photons in hot hadronic matter and present numerical parametrizations for the production rates for the use in dynamical calculations.

II. PHOTON PRODUCTION FROM HOT HADRONIC MATTER

Photon production from hot hadronic matter has been calculated by Kapusta *et al.* [6] with a simple effective model for hadrons. This study has been motivated by the need to decide whether the spectra of single photons produced in high energy nucleus-nucleus collisions can tell us anything about the formation of quark-gluon plasma in the early stage of the collision. However, the authors found that ''the hadron gas shines just as bright as the quark-gluon plasma.'' Moreover, it has later been pointed out that photon production from reactions including axial-vector mesons dominates that from the processes considered in Ref. [6] in hot hadronic matter [24]. The same conclusion has been obtained from an extended calculation based on a chirally symmetric effective Lagrangian with vector and axial-vector mesons [25]. This implies that the photon spectra, especially for photons with $E_\gamma < 3$ GeV, are dominated by the hadronic sources and provide information only on the hadronic phase in collisions. We summarize the results for various reactions and numerical parametrizations of them in the Appendix. The same conclusion holds true even when we include the space-time evolution of the hot and dense system produced in heavy-ion collisions [16,26]. However, the medium effects on the properties of mesons have not been addressed in these calculations.

In hadronic matter at high temperature and/or density we expect that properties of hadrons, such as effective masses and decay widths, are modified because of the phase transition and crossover into the deconfined phase of hadronic matter. Even below the phase transition temperature, chiral symmetry is expected to be partially restored, i.e., the magnitude of the order parameter $\langle \bar{q}q \rangle$ is reduced from its vacuum value. It has been suggested that the effective masses of vector mesons (m_ρ) would be reduced in hot dense matter according to a universal scaling law as [11]

$$\frac{m_\rho^*}{m_\rho} \approx \frac{m_N^*}{m_N} \approx \frac{f_\pi^*}{f_\pi}, \tag{1}$$

where m_N is the nucleon mass, f_π is the pion decay constant, and * indicates the in-medium value of the corresponding physical quantity. These changes have significant impact on the hadronic observables as well as on electromagnetic probes [27]. Recently it has been shown that the enhanced low mass dileptons observed by the CERES experiment can be well described using a ''dropping vector-meson mass'' in medium [10].

Photon production from hot dense matter will also be affected by the change of the properties of vector and axial-vector mesons in medium. Here we are interested in the effects of ''dropping masses'' of vector and axial-vector mesons in medium on photon production. To see these effects, we consider thermal production rates of photons from hadronic matter at a given temperature but with reduced masses. Since we assume that the pion mass does not change in medium, the in-medium mass of the vector meson is never less than $2m_\pi \approx 300$ MeV in the following calculations.

First we consider two scattering channels for photon production in hot hadronic matter. These reactions have been shown to be dominant sources of photons with $E_\gamma < 3$ GeV in hot hadronic matter. In Fig. 1 we show the thermal production rate of photons in $\pi + \rho \to \pi + \gamma$ reactions with four different values of the vector-meson mass at $T = 160$ MeV. We use Weinberg's mass formula for the effective masses of axial-vector mesons in medium, $m_{a_1}^* = \sqrt{2} m_\rho^*$. We can see that the production rate increases as the effective masses of vector and axial-vector mesons are reduced. We have more than an order-of-magnitude increase at $E_\gamma \approx 0.5$ GeV with $m_\rho = 300$ MeV. The enhancement in production rates can be understood as there are more thermal vector mesons with reduced masses and the cross section increases with in-medium masses. The shape of the spectra does not change much, except a shift of the peak to the low-energy region. Figure 2 shows the results for $\pi + \pi \to \rho + \gamma$ reactions. Even though the absolute magnitude is slightly less than in the previous case and these spectra are convex from below, we can reach a similar conclusion for $E_\gamma \geqslant 0.5$ GeV. We observe enhanced photon production rates with reduced effective masses of mesons.

On the other hand, we have opposite results for the decay channels. In Fig. 3 we show the effect of using the in-medium mass of mesons for the reaction $\rho \to \pi + \pi + \gamma$. The thermal production rates are reduced with medium effects.

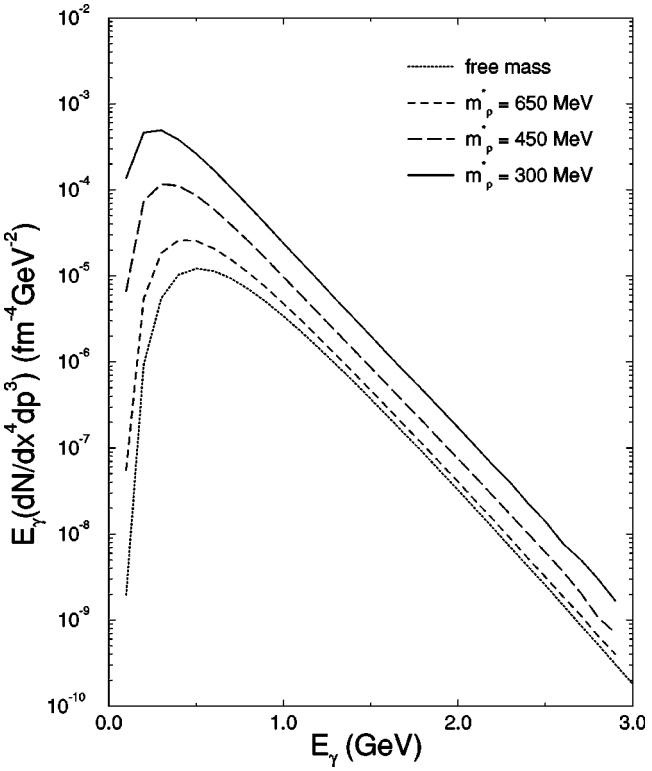

FIG. 1. Medium effects on the thermal emission rates of photons for the reaction $\pi\rho\rightarrow\pi\gamma$. We use $T=160$ MeV and four different values for the in-medium vector meson mass $m_\rho=300$, 450, 650, and 770 MeV from the top.

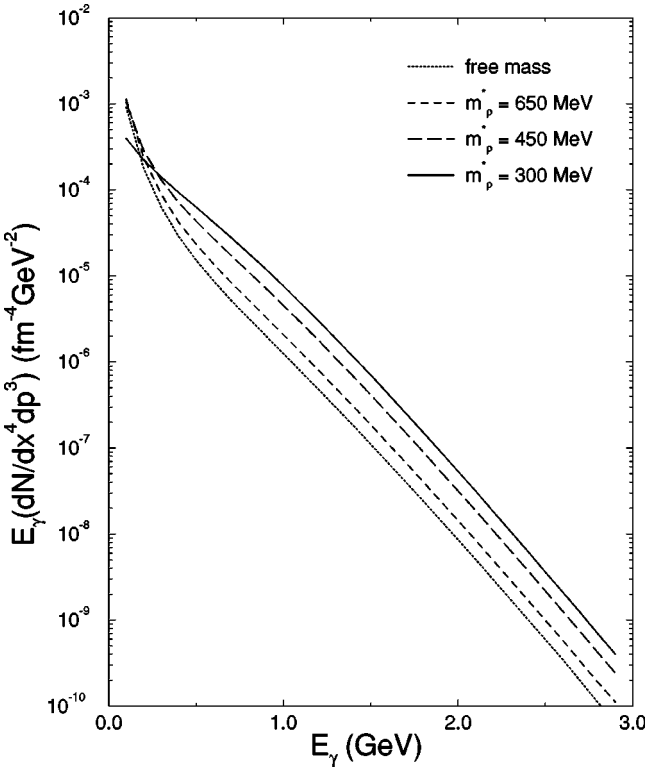

FIG. 2. Medium effects on the thermal emission rates of photons for the reaction $\pi\pi\rightarrow\rho\gamma$. The meaning of the curves is the same as in Fig. 1.

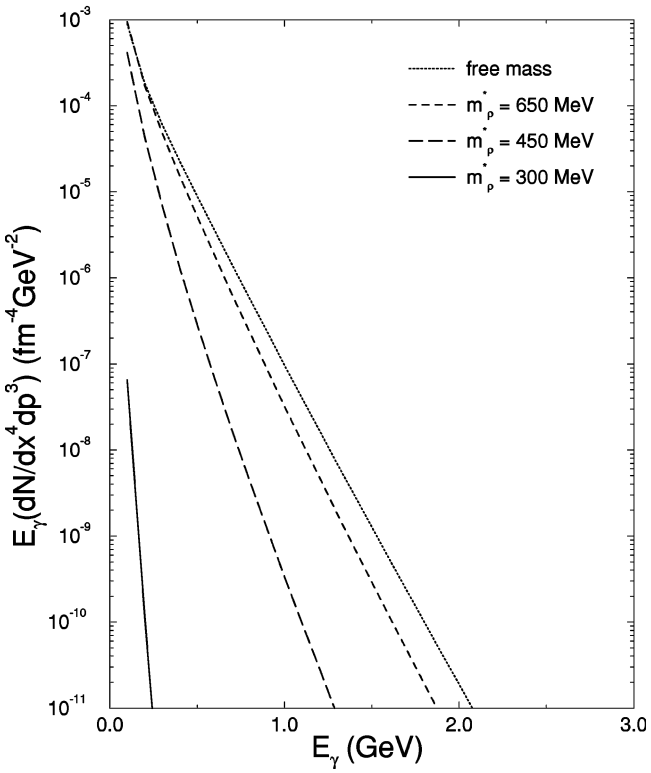

FIG. 3. Medium effects on the thermal emission rates of photons for the reaction $\rho\rightarrow\pi\pi\gamma$. The meaning of the curves is the same as in Fig. 1.

This is simply because of the reduced phase space of decay processes as the mass of vector mesons decreases. Because of their long lifetime, ω mesons decay outside the medium with their free mass. However, as we assume thermal equilibrium in the present calculation, the ω contribution remains small, in contrast to Ref. [20]. The η' radiative decay has a significant contribution below 0.5 GeV only. Since the contribution from the decay channels is relatively small compared to that from scattering channels, we neglect the decay channels in the following.

From these calculations we conclude that the total thermal production rates of photons increase with reduced vector and axial-vector meson masses. The production rate may be enhanced by 1 to 2 orders of magnitude. Similar rate enhancements have been found in the model-independent analysis of Ref. [17], where it is also pointed out that a finite pion chemical potential leads to further rate enhancement. Thus, it is very interesting to ask whether we can see such an enhancement in the observed photon spectra in high-energy nucleus-nucleus collisions. To answer this question, we need to include the space-time evolution of the hot dense matter produced in nuclear collisions.

III. MEDIUM EFFECT IN EXPANDING HOT DENSE MATTER

In the previous section we have shown that reduced in-medium masses of vector and axial-vector mesons lead to an enhancement in the thermal production rate of photons by 1 to 2 orders of magnitude. Since photon data appear to be consistent with earlier calculations with free masses, it is

interesting to see in a model whether these medium effects can be expected to survive in the observable photon spectra. In order to get the inclusive photon spectra for comparison to experimental data, we need to integrate the production rates over the space-time development of the expanding hot dense matter,

$$E_\gamma \frac{dN}{d^3p} = \int d^4x \left[E_\gamma \frac{dN}{d^4x d^3p}(E_\gamma, T, \mu) \right], \tag{2}$$

where T, μ indicate the temperature and density (chemical potential) dependence of the photon production rates. Thus, observable spectra also depend on the details of space-time evolution, on initial conditions, and on properties of the phase transition expected in hot dense matter.

In our calculation we assume a boost-invariant longitudinal expansion of the hot dense matter and use a fluid-dynamical description for the expanding system. The evolution of the system is governed by the conservation laws for energy and momentum,

$$\partial_\mu T^{\mu\nu}(x) = 0. \tag{3}$$

In the absence of dissipation, the energy-momentum tensor $T^{\mu\nu}$ is given by

$$T^{\mu\nu} = (\epsilon + P) u^\mu u^\nu - P g^{\mu\nu}, \tag{4}$$

where ϵ, P, and u^μ represent energy density, pressure, and local four-velocity of the medium, respectively. Further, we assume that density effects on photon production other than effects of the effective masses of vector and axial-vector mesons are negligible [20].

Using a simple one-dimensional hydrodynamic expansion with Bjorken's initial conditions [23], the transverse momentum distribution of photons (transverse momentum spectrum) at central rapidity is given by

$$\frac{dN}{dp_t dy}(y=0) = \pi R_A^2 \int \tau d\tau \int d\eta \left[E_\gamma \frac{dN}{d^4x d^3p}(E_\gamma, T) \right], \tag{5}$$

where τ is the proper time, R_A is the transverse size of the system, and η is the space-time rapidity. The proper time τ can be found as a function of temperature from the conservation of entropy as

$$\tau s(T) = \text{const}, \tag{6}$$

where s denotes the entropy density.

The dynamical properties of the expanding system—initial temperature, phase-transition temperature, and the lifetime of the mixed phase if there is a phase transition—depend on the details of how the vector-meson mass is changed in medium. To see the quantitative effect of the reduced in-medium mass on the photon production we consider two extreme cases: one in which the bulk of the change in the effective mass happens close to the critical temperature of a first-order phase transition (case A), and another with a more gradual change, where the effective mass starts to decrease significantly already at around a temperature $T = 100$ MeV (case B). The simple parametrizations for these two effective-mass scenarios are displayed in Fig. 4. In both cases we assume that the vector meson mass is not less than twice the pion mass, $m_\rho^* > 300$ MeV, even at very high temperatures. For axial-vector mesons we assume that the relation $m_{a_1}^* = \sqrt{2} m_\rho^*$ holds for the entire evolution.

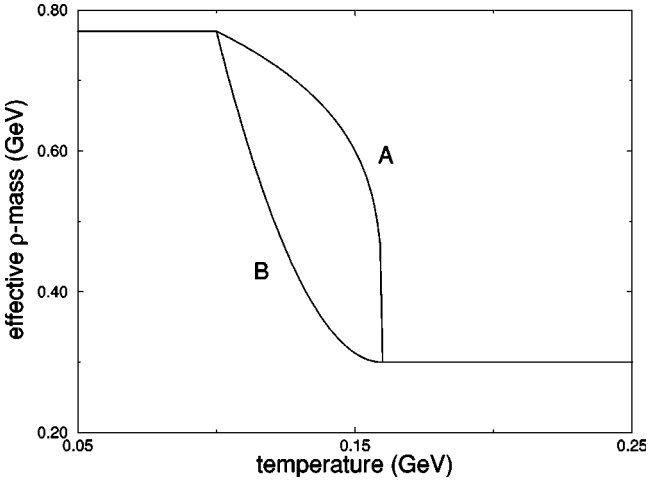

FIG. 4. Effective masses of vector mesons in medium. We consider two different mass profiles A and B as explained in the text.

Transverse expansion is neglected in the present work. The effect of transverse expansion on thermal photon production was found to be important for the apparent temperature of the spectra [16]. However, the goal of this investigation is to see whether there is a difference between a calculation with in-medium masses versus one with free masses. To isolate this effect a simple model without transverse expansion is sufficient. Similarly, a more refined treatment of freeze-out [28] is unnecessary as it would influence both calculations the same way.

A. No phase transition

First we determine the initial temperature of the system. This can be obtained from entropy conservation. If pions carry most of the system's entropy at freeze-out, entropy conservation relates the initial entropy density to the total observed pion rapidity density (including charged and neutral pions). Using the fact that the entropy and particle for an ideal massless boson gas is 3.6, one obtains

$$\pi R_A^2 \tau_0 s(T_0) = 3.6 \frac{dN_\pi}{dy}, \tag{7}$$

where τ_0 is the initial proper time and T_0 is the initial temperature. In this paper we use $\tau_0 = 1$ fm/c. Since we assume no phase transition, the initial entropy is given by the hadronic content of the system. Treating the hadronic matter as a noninteracting gas of hadrons, the entropy is given by

$$s_H(T) = \frac{1}{T}[\epsilon_H(T) + P_H(T)], \tag{8}$$

with

$$\epsilon_H = \sum_i \frac{g_i}{(2\pi)^3} \int d^3p \frac{\omega_i}{\exp(\omega_i/T) - 1}, \tag{9}$$

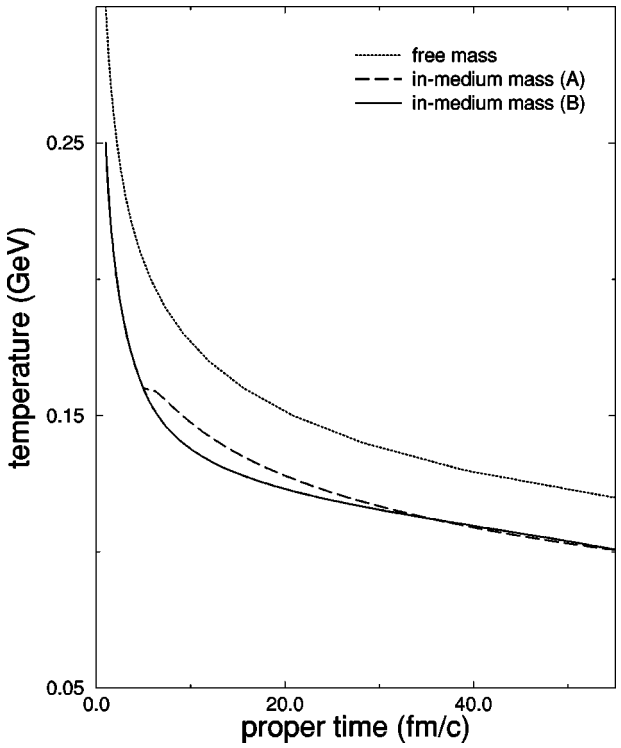

FIG. 5. Temperature evolution of the system with no phase transition. The dotted curve is the result obtained with free mass. The dashed curve is the result with in-medium masses for vector mesons in scenario A of Fig. 4. The solid curve is the result with in-medium masses for vector mesons in scenario B of Fig. 4.

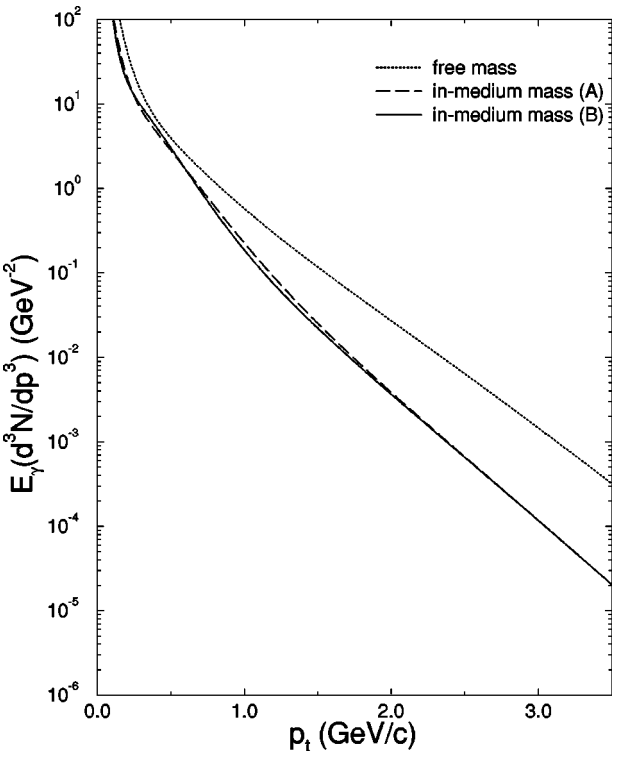

FIG. 6. Photon yield for a central ^{32}S+Au collision at 200A GeV with no phase transition. The meaning of each curve is the same as in Fig. 5.

$$P_H = \sum_i \frac{g_i}{(2\pi)^3} \int d^3p \frac{p^2}{3\omega_i[\exp(\omega_i/T)-1]},$$

where the sum is over various boson species that the system is composed of, g_i is the degeneracy factor, and $\omega_i = \sqrt{p^2+m_i^2}$.

For the central collisions of S+Au at 200 GeV/nucleon at the CERN SPS, we get $T_0 \approx 300$ MeV with free masses for vector and axial-vector mesons. We have assumed that the hadronic phase consists of π, η, ρ, ω, and a_1 mesons. This value of the initial temperature seems to be rather high for a hadronic phase. On the other hand, the initial temperature of the same system reduces to $T_0 \approx 250$ MeV assuming that the effective masses of vector mesons in medium reach the value shown in Fig. 4 at high temperature.

The temperature evolution, as the system cools down, is obtained from the entropy conservation equation

$$\tau s(T) = \tau_0 s(T_0). \tag{10}$$

In Fig. 5 we show the time dependence of the temperature with reduced in-medium masses for vector and axial-vector mesons according to scenarios A and B displayed in Fig. 4. The results are compared to the temperature evolution for the same system but with free masses. Interestingly, details of mass changes do not influence the temperature evolution very much. The initial mass of the vector meson has the only important effect on the evolution. At the very early stage of the evolution $\tau < 5$ fm/c, the temperature changes in the same way for both mass profiles A and B. When the effective mass changes suddenly as in scenario A, there is an early time interval without significant temperature change, resembling a first order phase transition in its effects. The system continues to cool down until it reaches the freeze-out temperature. In this paper we take the freeze-out temperature $T_f = 100$ MeV. As mentioned earlier, we have a lower initial temperature for a system with reduced masses compared to the value obtained with free masses. Furthermore, we can see that, in the entire evolution, the temperature of a system with reduced vector and axial-vector meson masses remains below the temperature of a system without medium effects on the effective masses.

These two medium effects, lower temperature at the beginning and in fact throughout the evolution, play significant roles in shaping the photon spectra from expanding hadronic matter. We show the results for the inclusive photon spectra obtained with reduced masses (two different profiles) in Fig. 6, and compare them to the results obtained with free masses. The in-medium effective mass induces a decrease in the production of inclusive photons, which is opposite to the effects of reduced masses on the thermal production rates of photons in the previous section. For photons with $p_t > 1$ GeV/c, total production is reduced by an order of magnitude with reduced in-medium masses. This indicates the importance of the reduced initial temperature and of the lower temperature of the system during the entire evolution compared to that of a system with free masses. Even though the thermal production rates increase with ''dropping effective masses,'' the increase is more than compensated by the reduced temperature of the system. The details of the mass evolution have no significant effect on the photon production since most photons are produced at the very early stage of

the evolution when there is no difference between the two mass profiles.

B. First-order phase transition

In contrast to the previous subsection, here we assume that the strongly-interacting matter produced in high-energy central collisions is in the quark-gluon plasma phase at the early stage of the evolution. Further, we assume that the system transforms into the hadronic phase through a first-order phase transition as it expands and cools down. In this case the initial conditions are determined by the properties of quarks and gluons. Including massless up and down quarks and gluons, we have for the initial temperature

$$T_0=\left(3.6\frac{dN_\pi}{dy}\,\frac{1}{\tau_0\pi R_A^2}\,\frac{1}{(4/3)(37\pi^2/30)}\right)^{1/3}. \tag{11}$$

For the system produced in S+Au collisions at the CERN SPS, using the value of dN_π/dy from the WA80 experiment, we get $T_0=203$ MeV.

The critical temperature can be determined by the pressure balance requirement

$$P_H(T_c)=P_Q(T_c). \tag{12}$$

The pressure in the quark-gluon plasma phase is given by

$$P_Q(T)=37\left(\frac{\pi^2}{90}\right)T^4-B, \tag{13}$$

where B is the bag constant and we use $B=206$ MeV [29]. In the hadronic phase the pressure is given by Eq. (9) with in-medium masses. Thus, the critical temperature depends on the effective masses of vector and axial-vector mesons. As we include the reduced effective masses of mesons, we get higher values for the critical temperature $T_c=160$ MeV, compared to $T_c=150$ MeV obtained with free masses.

In Fig. 7 we show the temperature evolution assuming a first-order phase transition. We consider the medium effect on the vector mesons with the two different profiles A and B, and compare the results to the evolution obtained with free masses. The evolution of the temperature in the plasma phase is given by

$$T(\tau)=T_0(\tau_0/\tau)^{1/3}, \tag{14}$$

until the system reaches the phase transition temperature at time $\tau_1=(T_0/T_c)^3\tau_0$.

In the mixed phase the temperature does not change, but the entropy changes by converting quark-gluon plasma to hadronic gas. The mixed phase continues to time τ_2 which is given by

$$\tau_2=r\,\tau_1, \tag{15}$$

where r is given by the ratio of the entropy densities in the two phases at the critical temperature, $r=s_q(T_c)/s_h(T_c)$ [5]. Thus, the lifetime of the mixed phase also strongly depends on the vector and axial-vector meson masses in medium. We find that the lifetime of the mixed phase is considerably reduced in the ''dropping mass'' scenario. With free masses the mixed phase continues for $\Delta\tau_{\rm mix}=20$ fm/c. However, this time is reduced to $\Delta\tau_{\rm mix}=5$ fm/c when we use in-medium masses. This implies that there might be no first-order phase transition as the effective masses of vector mesons are reduced further in medium, as discussed in Ref. [30]. Since the entropy difference between the two phases decreases as the masses are reduced in the hadronic phase, the system transforms very rapidly from the plasma phase to the hadronic phase. This is why we have a very short time for the mixed phase with ''dropping masses.''

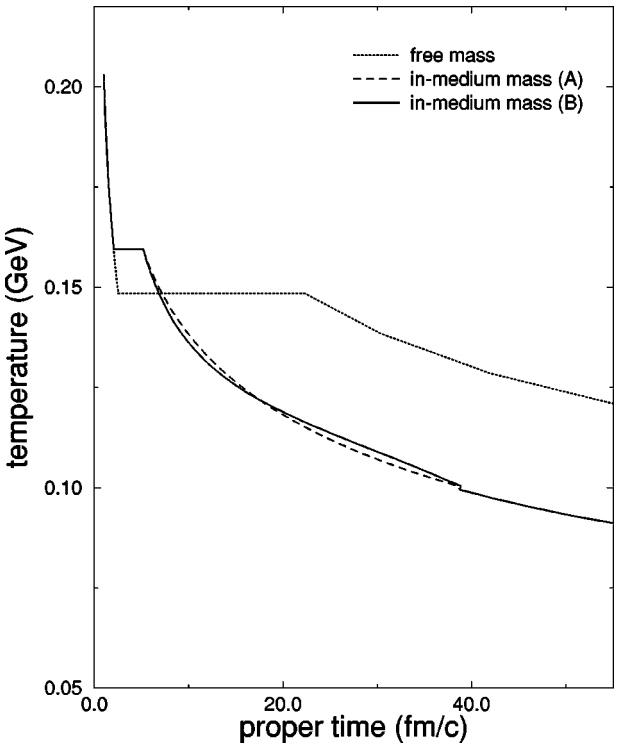

FIG. 7. Temperature evolution of the system with a first-order phase transition. The meaning of each curve is the same as in Fig. 5.

In the hadronic phase the evolution is given by Eq. (10) with T_c and τ_2 instead of T_0 and τ_0, respectively. As shown previously, the details of the temperature evolution do not depend strongly on how the effective masses of vector mesons change in medium. The hadronic phase soon cools down and the temperature of the system becomes lower than that for the system with free masses throughout most of the evolution. As a result, the system reaches the freeze-out temperature earlier than with free masses. The entire lifetime of the hot dense matter becomes short when we include the medium effects on the vector and axial-vector mesons.

Now we consider medium effects on the inclusive photon spectra from hot dense matter. In Fig. 8 we show the results with medium effects when a phase transition is assumed, and compare them to those obtained with free masses. The enhancement shown in the thermal production rates is compensated to some extent by the reducing effects from the changes in dynamic properties of the expanding system. Because of the short lifetime of the mixed phase there is a slight reduction in photon production from the plasma component of the mixed phase. However, the dominant contribution comes from the hadronic phase and the hadronic component of the mixed phase. These hadronic contributions show a significant increase because of the reduced masses, even

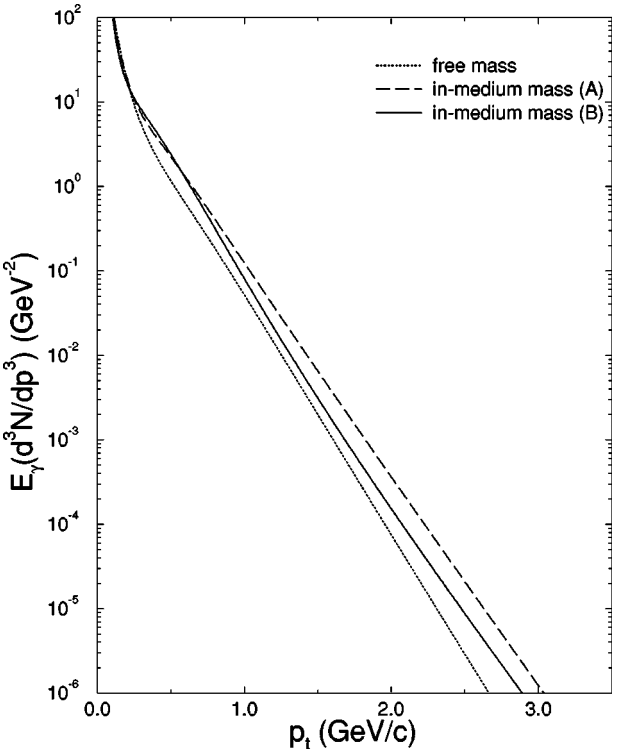

FIG. 8. Photon yield for a central ^{32}S+Au collision at 200*A* GeV with a first-order phase transition. The meaning of each curve is the same as in Fig. 5.

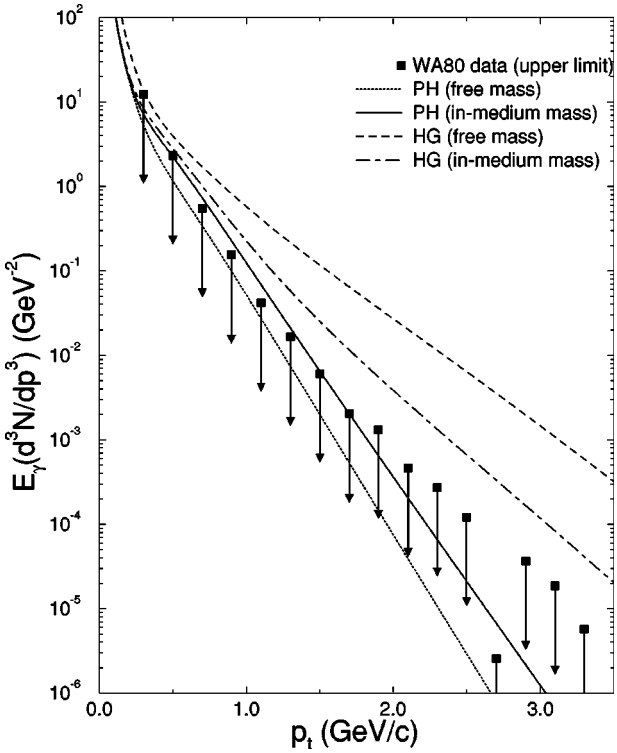

FIG. 9. Comparison with the WA80 upper limits. Dashed and dash-dot curves are for the results obtained in pure hadronic phase (with no phase transition) without and with medium effects A, respectively. Dotted and solid curves are for the results obtained assuming a first-order phase transition without and with medium effects A, respectively.

though there are reducing effects of the low temperature of the system and of the short lifetime of the mixed phase. This is because most of the hadronic contribution now comes from a high temperature. Also, we can see a rather apparent difference between scenarios A and B, and compared to the results obtained with no phase transition. We have more photons with scenario A than with scenario B. This is because of the difference in cooling rates of the system. The cooling rate is given by

$$\frac{dT}{d\tau} \sim \left[\frac{1}{(s(T))^2} \frac{ds(T)}{dT} \right]^{-1}. \tag{16}$$

It turns out that this cooling rate is ≈ 3 times slower with mass profile A than with mass profile B at the early stage of the expansion when the temperature decreases from 160 MeV to 140 MeV.

Finally, we compare our results to the upper limits obtained by the WA80 experiment in Fig. 9. We find that the purely hadronic scenario is excluded by these upper limits in our simple model even though we have an improved result with reduced masses. This is because of the rather high initial temperature of the system. However, we cannot rule out that a hadronic model using more degrees of freedom and a more realistic equation of state can be made consistent with the experimental information [31]. Our results are consistent with the WA80 upper limits if a first-order phase transition is assumed in the model [16]. The medium effects due to the ''dropping masses'' of vector mesons do not change these results much, except an increase in production rates for high p_t photons. We carried out a similar comparison with the preliminary WA98 data [3], reinforcing that the data are inconsistent with a pure hadronic calculation, while the assumption of a first-order phase transition leads to a reasonable description even with medium effects. The main conclusion of this article is that the data are still well-described in our simple model approach (with a first-order phase transition) without further modification when the medium effects of reduced masses are included.

IV. CONCLUSION

We have studied photon production from hot dense matter as a probe of the properties of hadrons in medium. We are interested in the effect of the reduced masses of vector and axial-vector mesons. Such a reduction has been suggested as a precursor phenomenon to the chiral phase transition. This has been very interesting recently, since the enhancement of low-mass dileptons observed in the CERES and HELIOS experiments at the CERN SPS can be well described assuming ''dropping masses'' of vector mesons.

First we have calculated thermal production rates of photons from hadronic matter at a given temperature but with reduced masses. It has been shown that the reduced mass increases the production rates by an order of magnitude at $T=160$ MeV for both reactions $\pi\rho \to \pi\gamma$ and $\pi\pi \to \rho\gamma$. However, the contribution from decay processes of vector mesons decreases with reduced effective masses simply because of the shrinkage of the phase space.

In order to compare with experimental data we have included the space-time evolution of the system as well as the

changes of masses in medium. For the evolution of hot dense matter we used a one-dimensional hydrodynamic expansion and considered cases with and without a phase transition. This model is clearly too simple to describe the complicated system produced in nuclear collisions, but is sufficient to understand, rather qualitatively, medium effects on photon production. We find that not only the thermal production rates of photons, but also the initial conditions and phase-transition properties of the system depend on the changes of the effective masses of vector and axial-vector mesons.

Assuming no phase transition, we have a relatively low value for the initial temperature with reduced masses $T_0 = 250$ MeV, because of the dependence of the initial entropy density of the system on the effective masses of vector and axial-vector mesons. Moreover, the temperature of the system with reduced masses is lower than that of the system with free masses throughout the evolution, which leads to an earlier freeze-out in the system with reduced masses. The inclusive photon spectra from hot dense matter produced in nuclear collisions are subject to two medium effects: enhancement from reduced masses of vector and axial-vector mesons and suppression from the changes in initial conditions and temperatures of the system. The suppression effects overwhelm enhancement and lead to a reduction of the spectra by an order of magnitude for high energy photons.

When we assume that there is a first-order phase transition in the system, the initial temperature is decided by the properties of quarks and gluons and not affected by the medium effects on the vector meson mass. The phase transition temperature and the time spent in the mixed phase, however, depend on the reduced meson masses. We find that the reduced effective masses change the phase transition temperature by about 10 MeV. The lifetime of the mixed phase strongly depends on the effective masses of vector mesons. It turns out that $\Delta\tau_{\rm mix}\approx 5$ fm/c with $m_\rho = 300$ MeV at $T = T_c$, which is considerably shorter than $\Delta\tau_{\rm mix}\approx 20$ fm/c with free masses. These changes reduce photon production and compensate the enhancement of thermal production rates with reduced masses. The final results, however, show slightly enhanced photon production since most photons are produced at the early stage of the hadronic phase in which the temperature is higher and the vector meson mass is smaller than in the system with free masses.

A comparison with experiments shows that our results are consistent with the experimental information assuming a first order phase transition, even though we include the medium effects from ''dropping masses'' of vector mesons.

In conclusion, thermal production rates of photons strongly depend on the changes in effective masses of vector and axial-vector mesons. However, these medium effects also change many important aspects of the dynamics of the expanding system. When we include these effects together, it is very hard to distinguish medium effects in the inclusive photon spectra observed at CERN SPS.

ACKNOWLEDGMENTS

We thank Terry Awes for discussions of the experimental situation. This work was supported in part by the U.S. DOE Grant No. DE-FG02-86ER40251.

APPENDIX

The thermal emission rates of photons have been calculated from relativistic kinetic theory. For a reaction $1+2 \rightarrow 3+\gamma$,

$$E_\gamma \frac{dN}{d^4x d^3p} = \frac{\mathcal{N}}{2(2\pi)^3}\int \frac{d^3p_1}{(2\pi)^3 2E_1}\frac{d^3p_2}{(2\pi)^3 2E_2}\frac{d^3p_3}{(2\pi)^3 2E_3}(2\pi)^4\delta^{(4)}(p_1+p_2-p_3-p)|\overline{\mathcal{M}}_i|^2 f_1(E_1)f_2(E_2)[1+f_3(E_3)]. \tag{A1}$$

Here (E^j,p^j) is the four-momentum of the $j^{\rm th}$ particle, (E_γ,p) stands for the photon, and the f's are Bose-Einstein or Fermi-Dirac distributions for each particle. $\mathcal{M}_i$ denotes the scattering amplitude for the given reaction, which is averaged over initial states and summed over final states to obtain $|\overline{\mathcal{M}}_i|^2$. The overall degeneracy factor $\mathcal{N}$ depends on the particular process. It is convenient to introduce invariant variables $s=(p_1+p_2)^2$ and $t=(p_1-p_3)^2$. After integrating over angles the integration reduces to four dimensions,

$$E_\gamma \frac{dN}{d^4x d^3p} = \frac{\mathcal{N}}{16(2\pi)^7 E_\gamma}\int_{s_0}^{\infty} ds \int_{t_{\rm min}}^{t_{\rm max}} dt |\overline{\mathcal{M}}_i|^2 \times \int_{[A]} dE_1 \int_{[B]} dE_2 f_1(E_1) f_2(E_2) \times [1+f_3(E_1+E_2-E_\gamma)]\frac{1}{\sqrt{aE_2^2-2bE_2+c}}, \tag{A2}$$

which can be integrated numerically. The details of notation are given in Ref. [25].

In the following we show numerical parametrizations for thermal production rates of photons obtained with axial-vector mesons included [25]. A parametrization is found by expressing the rate as a function of $\exp(-E_\gamma/T)$ and of dimensionless parameters like $x=T/m_\pi$ and $y=E_\gamma/m_\pi$. For the reaction $\pi\pi\rightarrow\rho\gamma$ we have

$$E_\gamma \frac{dN_{\pi\pi\rightarrow\rho\gamma}}{d^4x d^3p} = T^2 \exp(-E_\gamma/T) F_{\pi\pi\rightarrow\rho\gamma}(x,y), \tag{A3}$$

where

$$\begin{aligned} F_{\pi\pi\rightarrow\rho\gamma} = \exp[&-12.055+4.387x+(0.3755+0.008\,26x)y \\ &+(-0.007\,77+0.000\,279x)y^2 \\ &+(5.7869-1.0258x)/y \\ &+(-1.979+0.58x)/y^2]. \end{aligned} \tag{A4}$$

We obtain a similar parametrization for the reaction $\pi\rho\pi\rho\rightarrow\pi\gamma$ given by

$$E_\gamma \frac{dN_{\pi\rho\rightarrow\pi\gamma}}{d^4x d^3p} = T^2 \exp(-E_\gamma/T) F_{\pi\rho\rightarrow\pi\gamma}(x,y), \quad \text{(A5)}$$

where

$$F_{\pi\rho\rightarrow\pi\gamma} = \exp[-2.447 + 0.796x + (0.0338 + 0.0528x)y + (-21.447 + 8.2179x)/y + (1.524\,36 - 0.385\,62x)/y^2]. \quad \text{(A6)}$$

Finally we consider the decay channels. For the reaction $\omega\rightarrow\pi\gamma$ we have the same result as in Ref. [6], since there is no correction due to the a_1 meson. For ρ decay into $\pi\pi\gamma$, the correction due to the a_1 meson is rather small compared to the reactions discussed earlier. The parametrization is given by

$$E_\gamma \frac{dN_{\rho\rightarrow\pi\pi\gamma}}{d^4x d^3p} = T^2 \exp(-E_\gamma/T) F_{\rho\rightarrow\pi\pi\gamma}(x,y), \quad \text{(A7)}$$

where

$$F_{\rho\rightarrow\pi\pi\gamma} = \exp[-6.295 + 1.6459x + (-0.4015 + 0.089x)y + (-0.954 + 2.057\,77x)/y]. \quad \text{(A8)}$$

[1] E. V. Shuryak, Phys. Rep. **61**, 71 (1980); L. McLerran, Rev. Mod. Phys. **58**, 1001 (1986).

[2] J. B. Kogut and D. K. Sinclair, Nucl. Phys. **B280**, 625 (1987).

[3] For recent reviews see *Quark Matter '96* [Nucl. Phys. **A590**, 1 (1996)]; *Quark Matter '97* [Nucl. Phys. A (to be published)].

[4] E. F. Feinberg, Nuovo Cimento A **34**, 39 (1976); E. V. Shuryak, Sov. J. Nucl. Phys. **28**, 408 (1978).

[5] K. Kajantie, J. Kapusta, L. McLerran, and A. Mekjian, Phys. Rev. D **34**, 2746 (1986); J. Cleymans, J. Fingberg, and K. Redlich, *ibid.* **35**, 2153 (1987).

[6] J. Kapusta, P. Lichard, and D. Seibert, Phys. Rev. D **44**, 2774 (1991).

[7] G. Agakichiev *et al.*, Phys. Rev. Lett. **75**, 1272 (1995); J. P. Wurm *et al.*, CERES/NA45 Collaboration, Nucl. Phys. **A590**, 103c (1995); A. Drees *et al.*, CERES/NA45 Collaboration, in *Proceedings of the International Workshop XXIII on Gross Properties of Nuclei and Nuclear Excitations*, edited by H. Feldmeier and W. Nörenberg (GSI, Darmstadt, 1995), p. 151.

[8] M. Masera *et al.*, HELIOS-3 Collaboration, Nucl. Phys. **A590**, 93c (1995); I. Kralik *et al.*, HELIOS-3 Collaboration, in *Proceedings of International Workshop XXIII on Gross Properties of Nuclei and Nuclear Excitations*, edited by H. Feldmeier and W. Nörenberg, (GSI, Darmstadt, 1995), p. 143.

[9] V. Koch and C. Song, Phys. Rev. C **54**, 1903 (1996).

[10] G. Q. Li, C. M. Ko, and G. E. Brown, Phys. Rev. Lett. **75**, 4007 (1995); Nucl. Phys. **A606**, 568 (1996).

[11] G. Brown and M. Rho, Phys. Rev. Lett. **66**, 2720 (1996).

[12] R. Rapp, G. Chanfray, and J. Wambach, Phys. Rev. Lett. **76**, 368 (1996); Nucl. Phys. **A617**, 472 (1997).

[13] C. Song and V. Koch, Phys. Rev. C **54**, 3218 (1996).

[14] K. Haglin, Phys. Rev. C **53**, 2606 (1996).

[15] R. Albrecht *et al.*, Phys. Rev. Lett. **76**, 3506 (1996).

[16] D. K. Srivastava and B. Sinha, Phys. Rev. Lett. **73**, 2421 (1994); N. Arbex, U. Ornik, M. Plümer, A. Timmermann, and R. Weiner, Phys. Lett. B **345**, 307 (1995); J. J. Neumann, D. Seibert, and G. Fai, Phys. Rev. C **51**, 1460 (1995); A. Dumitru, U. Katscher, J. A. Maruhn, H. Stöcker, W. Greiner, and D. H. Rischke, *ibid.* **51**, 2166 (1995).

[17] J. V. Steele, H. Yamagishi, and I. Zahed, Phys. Lett. B **384**, 255 (1996); Phys. Rev. D **56**, 5605 (1997).

[18] S. Sarkar, J. Alam, P. Roy, A. K. Dutt-Mazumder, B. Dutta-Roy, and B. Sinha, nucl-th/9712007.

[19] M. Halász, J. V. Steele, G. Q. Li, and G. E. Brown, nucl-th/9712006.

[20] G. Q. Li and G. E. Brown, nucl-th/9706076.

[21] A. Dumitru, M. Bleicher, S. A. Bass, C. Spieles, L. Neise, H. Stöcker, and W. Greiner, hep-ph/9709487.

[22] S. Weinberg, Phys. Rev. Lett. **18**, 507 (1967).

[23] J. D. Bjorken, Phys. Rev. D **27**, 140 (1983).

[24] L. Xiong, E. Shuryak, and G. Brown, Phys. Rev. D **46**, 3798 (1992).

[25] C. Song, Phys. Rev. C **47**, 2861 (1993).

[26] S. Chakrabarty, J. Alam, D. Srivastava, B. Sinha, and S. Raha, Phys. Rev. D **46**, 3802 (1992).

[27] G. E. Brown and M. Rho, Phys. Rep. **269**, 333 (1996).

[28] J. J. Neumann, B. Lavrenchuk, and G. Fai, Heavy Ion Phys. **5**, 27 (1997).

[29] C. Wong, *Introduction to High-Energy Heavy-Ion Collisions* (World Scientific, Singapore, 1994).

[30] G. E. Brown, A. D. Jackson, H. A. Bethe, and P. M. Pizzochero, Nucl. Phys. **A560**, 1035 (1993).

[31] J. Sollfrank, P. Huovinen, M. Kataja, P. V. Ruuskanen, M. Prakash, and R. Venugopalan, Phys. Rev. C **55**, 392 (1997); J. Cleymans, K. Redlich, and D. K. Srivastava, *ibid.* **55**, 1431 (1997).